Sustained underwater acoustic communications with environmental-based time-reversal

Lussac P. Maia, António Silva, and Sérgio M. Jesus

Citation: The Journal of the Acoustical Society of America **144**, EL262 (2018); doi: 10.1121/1.5058119
View online: https://doi.org/10.1121/1.5058119
View Table of Contents: http://asa.scitation.org/toc/jas/144/4
Published by the Acoustical Society of America

Maia *et al.*: JASA Express Letters https://doi.org/10.1121/1.5058119 Published Online 10 October 2018

Sustained underwater acoustic communications with environmental-based time-reversal

Lussac P. Maia
Instituto de Estudos do Mar Almirante Paulo Moreira, Rua Kioto, 253, Arraial do Cabo, Rio de Janeiro 28930-000, Brazil
lussac.maia@marinha.mil.br

António Silva and Sérgio M. Jesus
Laboratory of Robotics and Engineering Systems, Universidade do Algarve, Campus de Gambelas, Faro, PT8005-139, Portugal
asilva@ualg.pt, sjesus@ualg.pt

Abstract: The usage of time-reversal in underwater communications relies on array channel matched-filtering, coherent channel replica alignment and summation. Traditionally, replicas are channel responses to probe signals received at a previous time. These are noisy and subject to distortion due to channel variability. This paper offers an alternative where noisy and potentially distorted channel replicas are replaced by noise-free and time-updated replicas generated by a numerical model constrained on previously data-identified environmental parameters. The method is applied on real data, where a quadrature phase shift key modulated signal on a 25.6 kHz carrier at 4 kbit/s was transmitted in a shallow water area over a distance of approximately 900 m. Sustained analysis without supervision shows that the proposed method may attain a mean square error gain up to 5.4 dB when compared to traditional time-reversal.

[DRD]
Date Received: May 28, 2018 **Date Accepted:** September 15, 2018

1. Introduction

Underwater acoustic communications in shallow water are challenging because multiple reflections at the sea surface and in the seabed interact with a dynamic channel waveguide, where the channel impulse response (CIR) is characterized by time-frequency double spreading due to multipath propagation and time variability. The former causes severe inter-symbol interference while the latter causes signal time-compression or time-dilation and spectrum distortion, mainly due to sensor motion and unavoidable ocean dynamics. Coherent communications in this scenario require channel equalization to reach successful message recovery.

Among the techniques for underwater channel equalization found in the literature, decision feedback equalizers and their multichannel versions when a receiving array is available are the most commonly used.[1] The robustness and the stability of decision feedback equalizers largely depend on the complexity of the channel, known to be particularly severe in shallow water. This situation is aggravated in the multichannel case where one "bad channel" may spoil the whole channel equalization, and the computational burden increases the complexity of least squares and Kalman type adaptation algorithms on the order of the number of channels squared.[2] This is the main reason why passive time-reversal (PTR) has been introduced as a pre-processor for multi-channel equalization[3–5] and used with real data in orthogonal frequency-division multiplexed signals[6] and as a decision feedback equalizer pre-processor.[7,8] PTR is a low complexity receiver that uses multichannel probing for time signal refocusing, reducing time spread and improving inter-symbol interference. However, any lack of accuracy in the CIR identification can severely reduce its performance. Recognizing this key point, the authors proposed an alternative to data-driven CIR estimates by generating CIR replicas obtained as the output of a numerical propagation model.[9] Ideally, and if correctly set up, this model would allow generation of noise-free channel estimates and follow channel variability by using independent measurements of physical parameters, such as sound speed profile, surface roughness, source-receiver relative position, etc., if and when available. Correct setup means relatively tight search intervals over the most acoustically relevant parameters. So, assuming a suitable setup, this new technique couples PTR with environmental and model knowledge and is therefore termed as environmental passive time-reversal (EPTR).

In EPTR, at each time instant the CIR replica used for time-reversal is selected as the model output that best matches the pulse-compressed (PC) data driven CIR estimate. This selection process operates in a search space defined by a subset of the model physical parameters and in many respects is analogous to what is referred to in the literature as environmental focusing (EF).[10] Since the CIR replica is obtained as the output of deterministic model, it is noise-free and therefore advantageous for PTR in comparison to noisy CIR estimates generated by standard PC. However, this advantage is limited by unavoidable modeling mismatch. A central issue is whether replica noise can be advantageously traded for model mismatch. This letter provides insight into this issue, by performing a sustained test of EPTR on a real data set of over one hour of acoustic transmissions collected during the Underwater Acoustic Network experiment, conducted in a shallow water area near Trondheim, Norway, during May 27, 2011. Data blocks were transmitted by a Kongsberg cNode mini modem, on a carrier frequency of 25.6 kHz at a data rate of 4 kbit/s. The data were received on a 64-m long vertical array of hydrophones containing 16 elements, where the spacing between elements is 4 m. The array is placed 890 m away from the source. The results show that EPTR can outperform conventional PTR with a mean square error gain up to 5.4 dB, at an affordable computational cost.

This paper is organized as follows: the methodology for performance validation and the EPTR receiver structure are summarized in Sec. 2, the experiment and the results obtained are described in Sec. 3, and conclusions are drawn in Sec. 4.

2. Methodology and EPTR receiver structure

The methodology adopted in this work can be better understood with the help of the diagram of Fig. 1. The selector in position 1 implements the classical PTR receiver based on PC replica estimates. In position 2, the PC replica estimates are used to drive an intermediate optimization process dedicated to determine the numerical model output that "best" matches the PC replica. This optimization is carried out in the EF block that takes as input the *a priori* physical channel information and generates noise-free channel responses for PTR at the output—this constitutes the EPTR receiver. The PC block output is simply obtained as the correlation of the transmitted and the received probe signal, which provides the optimal channel impulse response estimate in the least square sense, under the following assumptions: (i) that the probe signal covers a sufficiently large frequency band to resolve the most closely spaced arrivals of the channel and (ii) that there is no channel variability during the estimation process. In practice, deviation from these assumptions (specially that of the channel variability) limits its applicability and thus the noise reduction obtained at the output of the PC block. In fact, the remaining noise at the PC output is the motivation for the EPTR, which objective is to produce a noise-free replica of the CIR that best matches the true channel.

This is the role of the EF block, that consists of an optimization procedure, where one CIR is selected among a set of possible replicas calculated by a numerical propagation model. In the EF block, the *a priori* physical parameters are used to define a search space ψ of possible combinations; then the ray trace numerical model Bellhop is exhaustively run for the environmental combinations on the search space and, finally, the obtained CIR replicas are matched to the noisy PC estimates using a broadband correlation function for a given snapshot, given by

$$B(\psi) = \frac{1}{L}\sum_{l=1}^{L} \frac{\|\mathbf{g}_l^H \breve{\mathbf{g}}_l(\theta_\psi)\|^2}{\|\mathbf{g}_l\|^2 \|\breve{\mathbf{g}}_l(\theta_\psi)\|^2}, \tag{1}$$

where $\breve{\mathbf{g}}(\theta_\psi)$ denotes the model predicted CIR conditioned on model parameter set θ_ψ generated from search space ψ, $\mathbf{g}$ denotes the observed CIR, subscript l is the

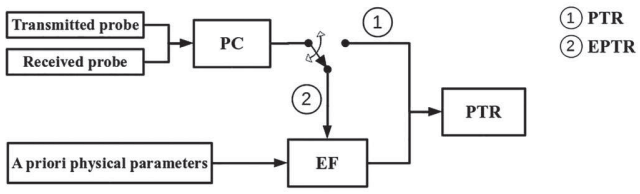

Fig. 1. Methodology to test EPTR and compare performance with classical PTR: two channel identification methods applied to time-reversal underwater communications: (1) pulse compression yielding the PTR and (2) EF with pulse compression yielding the EPTR.

hydrophone number, L is the number of hydrophones, and H denotes conjugate transpose. The CIR replica associated with the maximum of Eq. (1) is selected to be used for plain time-reversal in the PTR block as shown in Fig. 1. Time-reversal filtering—implemented in the PTR block—assumes a data model where the baseband transmitted signal $s[n] = \sum_i a[i]p[n - iT_s]$ crosses a channel with CIR $g[n, k]$, thus yielding the received signal given by $y[n] = \sum g[n, k]s[n - k] + w[n]$, where $w[n]$ denotes additive random noise, $a[i]$ is the symbol sequence, $p[n]$ is the pulse shape, and T_s is the sampling interval. Using the expected CIR $\hat{g}_l[n]$, either from PC in path 1 or that selected in the EF block along path 2 (of Fig. 1), one performs the conjugate time-reversal filtering and summing given by

$$z[n] = \sum_l a[n] * p[n] * g_l[n] * p[n] * \hat{g}_l^{\dagger}[-n] + w_l[n] * \hat{g}_l^{\dagger}[-n] * p[n]. \quad (2)$$

Disregarding the noise component, we can observe that the channel reduces to $Q[n] = \sum_l \sum_k \hat{g}_l^{\dagger}[k] g_l[n - k]$, the so-called PTR Q-function, having time duration and peak to side-lobe ratio that defines the success of the PTR receiver. Unfortunately PTR Q-function performance can not be exactly measured with real data.

3. Experimental results of the UAN11 sea trial

3.1 Environment and algorithm setup

The Underwater Acoustic Network project sea trial took place in the Strindfjorden, near Trondheim, Norway, in May 2011.[11] In this work, Quadrature Phase Shift Keying (QPSK) modulated data, transmitted during one hour late night on May 27, was used. During that data set the setup was as follows: a Kongsberg cNode Mini modem, acting as transmitting source, was suspended at 28 m depth, 890 m away from a 16-hydrophone 4 m-spacing vertical line array, with the first hydrophone located at 14.1 m depth. The water depth was approximately 38 m at the source and 98 m at the receiver array location, so the transmission channel was strongly range dependent downward propagating from source to receiver. Both the source modem and the receiving array were moored, so the only source-receiver depth-range variations were due to currents and tide. A conductivity-temperature-depth cast was made on May 27, generating the sound speed profile shown in Fig. 2(c), where one can notice that the depth of approximately 40 m acts as a turning point for the sound speed that is downward refracting above and upward refracting below, while there is an initial formation of a mixed layer above 20 m.

In order to develop the EPTR receiver, additional environmental information is necessary to setup the numerical model. This includes the bottom parameters that, in this case, were derived from historical information of the area, being characterized as a rock bottom covered by a 5 m thick sediment layer of mud and clay. The bottom and sediment parameters are listed in column "Reference" of Table 1. This table also shows in the last two columns, the search interval and the number of discrete points in the interval, respectively, for those parameters included in the EF optimization procedure which are those of source-receiver position and bottom sediment. The obtained search space has a total of 5000 points which is simply the product of the number of discrete points in the last column of Table 1 and is exhaustively searched during the EF optimization scheme.

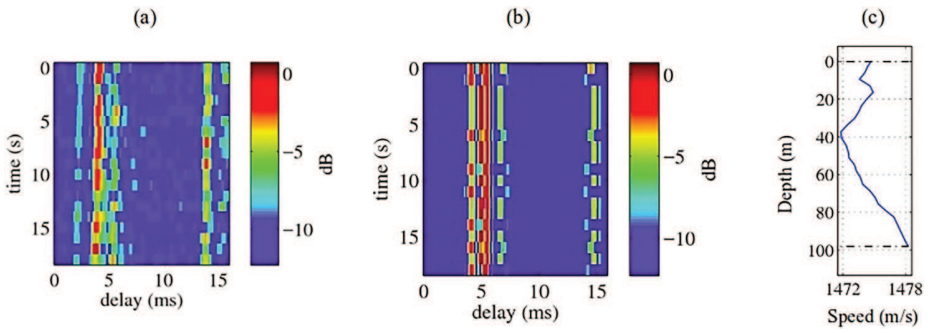

Fig. 2. (Color online) Channel impulse response variability over a data frame transmitted at time 23:54 on May 27, 2011, and received on the 42 m-depth hydrophone: using pulse compressing (a) and environmental focusing (b). Sound speed profile acquired on May 27 (c).

Table 1. Environmental physical parameters for propagation modeling and EF.

Physical parameter	Unit	Reference	Search	Size
Water column				
Source-receiver range	(m)	890	870–910	5
Source depth	(m)	28	26.50–29.50	5
Array depth	(m)	14.1	13.10–15.10	5
Sound speed profile	(m/s)	[see Fig. 2(c)]		
Sediment				
Thickness	(m)	5	—	—
Compression speed	(m/s)	1550	1480–1620	10
Compression attenuation	(dB/λ)	0.8	0.60–1.00	2
Density	(g/cm^3)	1.8	1.30–2.30	2
Bottom				
Compression speed	(m/s)	2100	—	—
Shear speed	(m/s)	250	—	—
Compression attenuation	(dB/λ)	0.1	—	—
Shear attenuation	(dB/λ)	2.5	—	—
Density	(g/cm^3)	2	—	—

3.2 Analysis and performance

The transmitted bit sequence was QPSK-modulated on a 25.6 kHz carrier with a bandwidth of 4 kHz and a bit rate of 4000 bits/s. The data are separated in frames where each frame has a preamble and a postamble with an m-sequence of 511 symbols, a header of 40 symbols and 20 messages composed of a 127 symbol m-sequence and 1873 symbols of data each. So, each data frame has approximately 37 000 data symbols. For the real data processed in this work, both the PTR and the EPTR receivers employ pre-processing based on standard signal resampling for compensation of any Doppler trend or transmitter/receiver clock impairment using the preamble and postamble, as well as post-processing for phase lock and recovery. The 127-symbol m-sequences are inserted in the payload at equal intervals of 1 s, and are used for channel tracking purposes. In this work, the PC-based CIR estimate, referred to in Sec. 2, is obtained as the mean CIR over the 20 s of each data frame. Figure 2 shows the estimated CIRs of one of the data frames acquired at 23:54 on May 27, 2011, with the plain PC method (a) and modeled after EF search (b). One may remark that there is a quite accurate tracking of the main features of the channel behavior along this short period of time, and also that the EF output has a noise floor level much lower than that of the PC estimate. There is a set of estimated environmental parameters as a by-product of the EF block, but these are irrelevant for the purpose of this paper.

In order to determine the ability of the proposed method to track the channel over time, Fig. 3 shows the mean square error comparative performance of PTR and

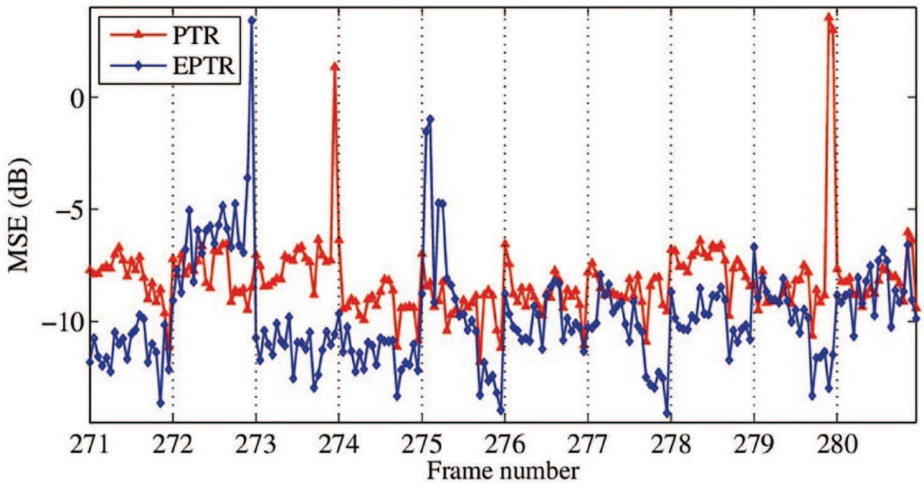

Fig. 3. (Color online) Mean square error of soft-decision recovered symbols obtained by EPTR (blue diamonds) and PTR (red triangles) along ten data frames with 20 messages of 1873-symbols-1-s long each. The start time corresponds to 22:52.03 of May 27.

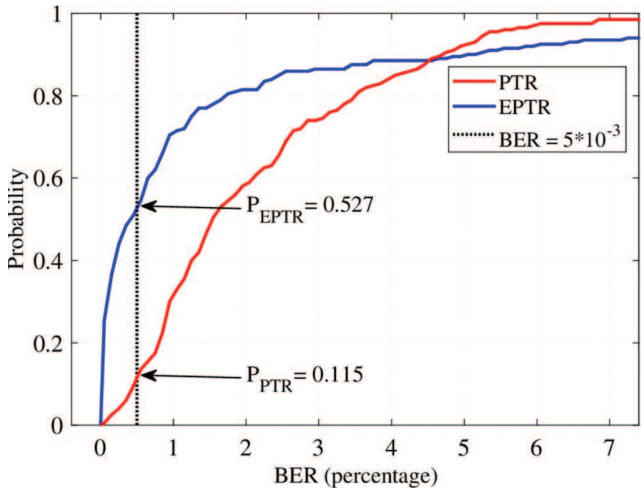

Fig. 4. (Color online) Empirical cumulative distribution function versus bit error rate (BER) in % for the EPTR (blue) and PTR (red) receivers, estimated from the 200 1873-symbol messages transmitted at 22:52:03 on May 27, during the Underwater Acoustic Network sea trial.

EPTR, in an unsupervised test of ten frames of 20 s each transmitted for a period of about 1 h between 22:52 and 23:56 on May 27, 2011. The mean square error was computed for each 1-s slot containing N symbols, being mathematically defined by $\epsilon = (1/N)\sum_{n=1}^{N}(s[n] - z[n])^2$, where $s[n]$ is a transmitted symbol sequence, $z[n]$ is the corresponding predicted symbol sequence. The ten 20-s frames were transmitted at regular intervals but are shown in this figure as a continuous data set, just separated by the vertical dotted lines. Each blue diamond, for EPTR, or red triangle, for PTR, represent a message containing 1873 QPSK symbols and there are 20 messages per frame. This figure indicates that EPTR clearly outperformed PTR in nine out of the ten frames. The results show that in these nine frames EPTR achieved a gain over PTR between a minimum of 0.39 and a maximum of 5.48 dB, with a mean gain of 2.61 dB. Only for data frame 272, EPTR failed to provide a consistent channel estimate.

The same result can be seen in another more practical user perspective in terms of bit error rate (BER) performance. Figure 4 shows the empirical cumulative distribution function versus BER estimated using the results of the 10 frames of 20-messages each (i.e., 200 samples). For interesting BER values below 1% the EPTR shows a clear upper hand over PTR and, as an example, the probability for BER $\leq 5 \times 10^{-3}$ is 0.52 for EPTR and only 0.11 for the PTR receiver.

4. Concluding remarks

The proposed EPTR method can be viewed as a pre-processor to improve time-reversal communications performance through the mitigation of the effect of noise in CIR estimation, by replacing the noisy channel estimates by noise-free acoustic propagation numerical modeled replicas obtained by EF. Results obtained with real data show the feasibility of the proposed method and suggest that EF, if driven with the appropriate prior search space of environmental parameters, can succeed to mitigate modeling error and reduce the inter-symbol interference in a EPTR receiver, yielding substantial and sustained gain without supervision, relative to the standard PTR. This gain translates into a much higher probability of reception for EPTR when compared to PTR, at low BER. These results somehow contradict the common belief that model-based methods are unable to cope with environment-induced channel variability in frequency bands useful for underwater acoustic communications. It is suggested that EPTR contributes as a step forward in the direction on understanding how physical modeling can be used to estimate and compensate real channels in underwater acoustic communications.

Acknowledgments

This work was funded by the Postgraduate Study Abroad Program of the Brazilian Navy, Grant No. Port.386/MB-07/13, and by European Commission Framework Program for Research and Innovation, through the grant for Strengthening Maritime Technology Research Center (STRONGMAR) project (Grant No. H2020-TWINN-2015, 692427). The authors thank the support of IEAPM-MB and LARSyS.

References and links

[1]M. Stojanovic, J. Catipovic, and J. Proakis, "Adaptive multichannel combining and equalization for underwater acoustic communications," J. Acoust. Soc. Am. **94**, 1621–1631 (1993).

[2]J. Preisig, "Adaptive multichannel decision feedback equalization using subarray processing," J. Acoust. Soc. Am. **131**(4), 3275 (2012).

[3]M. Stojanovic and L. Freitag, "Multiuser undersea acoustic communications in the presence of multipath propagation," in *Proceedings of the MTS/IEEE Oceans 2001*, 2165-69, Honolulu, HI, November 2001, pp. 2165–2169.

[4]J. Gomes, A. Silva, and S. M. Jesus, "Joint passive time reversal and multichannel equalization for underwater communications," in *Proceedings of the MTS/IEEE Oceans 2006*, Boston, MA, September 2006.

[5]J. P. Gomes, A. Silva, and S. M. Jesus, "Experimental assessment of time-reversed OFDM underwater communications," in *Proceedings of ECUA 2008*, Paris, France, July 2008.

[6]J. P. Gomes, A. Silva, and S. M. Jesus, "Adaptive spatial combining for passive time-reversed communications," J. Acoust. Soc. Am. **124**(2), 1038–1053 (2008).

[7]U. Vilaipornsawai, A. Silva, and S. M. Jesus, "Underwater communications for moving source using geometry-adapted time reversal and DFE: UAN10 data," in *Proceedings of the MTS/IEEE Oceans 2011*, Santander, Spain, June 2011.

[8]U. Vilaipornsawai, A. Silva, and S. M. Jesus, "Experimental testing of asymmetric underwater acoustic networks," in *Proceedings of the International Conference on Communications and Electronics ICCE 2014*, Da Nang, Vietnam, July 2014.

[9]L. P. Maia, A. Silva, and S. M. Jesus, "Environmental model-based time-reversal underwater communications," IEEE Access J. **6**(1), 10041–10051 (2017).

[10]M. D. Collins and W. A. Kuperman, "Focalization: Environmental focusing and source localization," J. Acoust. Soc. Am. **90**(3), 1410–1422 (1991).

[11]A. Caiti, K. Grythe, J. M. Hovem, S. M. Jesus, A. Lie, A. Munafo, T. A. Reinen, A. Silva, and F. Zabel, "Linking acoustic communications and network performance: Integration and experimentation of an underwater acoustic network," IEEE J. Ocean. Eng. **38**(4), 758–771 (2013).